Thermal Models to High Energy Collisions

Dawit Solomon Worku (PhD)

Department of Physics and Mathematics, Cape Peninsula

University of Technology (CPUT) Bellville Campus 7945, South Africa

August 27, 2019

Abstract

In order to understand nuclear matter at high temperatures and densities formed in heavy ion collisions, it is useful to use statistical-thermal models to analyze the final state. We apply different types of statistical distributions and discuss their effects.

We discuss the hadron resonance gas model and its extension to include the Hagedorn spectrum [1, 2, 3]. The Hagedorn temperature, T_H is determined from the number of hadronic resonances including all mesons and baryons. This leads to the result $T_H = 174\pm11$ MeV consistent with the critical and the chemical freeze-out temperatures at zero chemical potential. We apply this result to calculate the speed of sound and other thermodynamic quantities in the resonance hadron gas model for a wide range of baryon chemical potentials using the chemical freeze-out curve [4, 5]. We compare some of our results to those obtained previously [6, 7].

We have also made additions to THERMUS [8] by including charm and bottom hadrons from the particle data table [9]. Then, we analyze and discuss the hadronic abundances measured in proton-proton (p-p), gold-gold (Au-Au) and lead-lead (Pb-Pb) collisions at Relativistic Heavy-Ion Collider (RHIC) [10] and Large Hadron Collider (LHC) [11, 12, 13] experiments using THERMUS. The THERMUS results obtained with the 2002 particle data table and new particle data table (2008 particle data table) and their differences are discussed. In particular, the data from the RHIC experiment for Au-Au collisions at 130 GeV and 200 GeV [10] are discussed and analyzed. Similarly, using the preliminary particle yield results of p-p collisions at 0.9 TeV and 7 TeV as well as Pb-Pb collision at 2.76 TeV [11, 12, 13] are presented and the thermodynamic parameters are obtained from the fit are discussed.

Contents

0.1 Review of THERMUS

THERMUS is a package of C++ classes and functions allowing statistical thermal model analyzes. It is written by S. Wheaton [8] to be used within the ROOT [14] framework of analysis. The statistical thermal model assumes a hadron gas at chemical freeze-out.

There are other codes, e.g., the Statistical Hadronization with Resonances (SHARE) [15], which is also a collection of programs designed for the statistical thermal analysis of particle production in relativistic heavy ion collisions. With the input of intensive statistical parameters, it generates ratios of particle abundances. Another successful code is the Therminator: Thermal heavy-Ion generator [16]. It is an event generator designed for studying particle production in relativistic heavy ion collisions obtained at facilities such as the GSI, SPS, RHIC, and LHC, it uses the statistical thermal model. The program implements thermal models of particle production with a single thermal and chemical freeze-out temperature which coincide.

The following applications of THERMUS have been considered in the literature:

- The identification of the universal freeze-out criteria, have four conditions that have been investigated [5]; these are:

  - The Cleymans-Redlich freeze-out criterion, under this condition, the freeze-out condition occurs at a fixed energy per hadron, i.e., $E/N = 1$ GeV [17].

  - The Braun-Munzinger-Stachel freeze-out criterion, under this condition, the baryon density is fixed, i.e., $n_B + n_{\bar{B}} = 0.12$ fm^{-3} [18, 19].

  - Recently, it has been observed at fixed temperature-normalized entropy density, $s/T^3 = 7$ as freeze-out criterion [5, 20, 21, 22].

  - The percolation model of H. Satz [5, 23] has been put forward to describe the chemical freeze-out in heavy ion collisions at all

energies. The model is a self-consistent equation for the densities based on geometric estimates.

In particular, the sensitivity to such factors as collision system, excluded volume dependence, resonance spectrum mass cut-off, strangeness saturation and canonical strangeness corrections was determined.

- It can be used to generate particle yield predictions for the energy dependence of other thermodynamic quantities (i.e., number density, energy density, pressure and entropy), which have been defined in section **??**, and particle ratios.

- Speed of sound in a hadronic gas [24, 25].

THERMUS has three distinct thermal model formalisms. The first is grand-canonical ensemble, where baryon number (B), strangeness (S), charge (Q), charm (C) and bottom (b) are conserved on average. The next formalism is a strangeness-canonical ensemble in which strangeness is exactly conserved, while B, Q, C and b are treated grand-canonically, finally, a canonical ensemble in which B, S and Q are conserved exactly. Furthermore, it takes into account decay chains and detector efficiencies. These enable sensible fitting of model parameters to experimental data.

The source code of the THERMUS package is available in [8] and has been extended by S. Wheaton so that additional quantum numbers can be included in the code [1]; note that most of the additional particles are charm and bottom with the corresponding decay elements. It can treats charm and bottom grand-canonically. First, we will mention and state the statistical formalism for the extension of THERMUS, then proceed to explain how to use the 2008 particle data table and discuss the results and compare with previous results [26].

---

[1]The extended source code was written by S. Wheaton.

3

0.2   The Statistical Formalism

The hadron gas partition function contains all the thermodynamic information of the system. The choice of partition function depends on the statistical ensemble. Next, we shall use the grand-canonical ensemble in this chapter and implement it with the 2008 particle data table in THERMUS.

In the grand-canonical ensemble, there are several parameters to characterize the system. These are temperature, chemical potential, volume and non-equilibration factors. The hot dense matter produced in nucleus-nucleus collision is large enough to be described by the grand-canonical ensemble.

In the grand-canonical ensemble, energy and quantum numbers are conserved on average through the temperature, T and the chemical potentials, μ. The logarithm of the total partition function for a multi-component hadron gas of volume V and temperature T is given by

$$\ln Z^{GC}(T, V, \mu) \;\; = \;\; \sum_i \frac{g_i V}{(2\pi)^3} \int d^3 p \ln \left(1 \pm e^{-\beta(E_i - \mu_i)} \right)^{\pm 1}, \qquad (1)$$

where g_i and μ_i are the degeneracy and chemical potential of hadron species i, $\beta \equiv 1/T$, while $E_i = \sqrt{p^2 + m_i^2}$, with m_i being the particle mass. The plus sign refers to fermions and the minus sign to bosons.

In this ensemble, we considered the conservation of the quantum numbers i.e., B, S, Q, C and b. The chemical potential for hadron species i is given by

$$\mu_i \;\; = \;\; B_i \mu_B + S_i \mu_S + Q_i \mu_Q + C_i \mu_C + b_i \mu_b, \qquad (2)$$

where B_i, S_i, Q_i, C_i and b_i are the baryon, strangeness, charge, charm and bottom number, respectively, and μ_B, μ_S, μ_Q, μ_C and μ_b are the corresponding chemical potentials for the conserved quantum numbers. This ensemble is widely used in applications to heavy ion collisions [17, 27, 28, 29, 30, 31, 32,

33]. The fugacity for each of these chemical potentials is defined as $\lambda \equiv e^{\mu/T}$.

The density of hadron species i with quantum numbers B_i, S_i, Q_i, C_i and b_i, spin-isospin degeneracy factor g_i, and mass m_i, emitted directly from a fireball at temperature T is

$$n_i(T, \{\mu\}, \{\gamma\}) \;=\; g_i \int \frac{d^3 p}{(2\pi)^3} \left[\gamma_T \lambda_T e^{\sqrt{m_i^2 + p^2}/T} \pm 1 \right]^{-1}, \tag{3}$$

where

$$\{\mu\} = \{\mu_B, \mu_S, \mu_Q, \mu_C, \mu_b\}, \quad \{\gamma\} = \{\gamma_s, \gamma_c, \gamma_b\}, \quad \gamma_T = \gamma_s^{-|S_i|} \gamma_c^{-|C_i|} \gamma_b^{-|b_i|},$$

and

$$\lambda_T = \lambda_B^{-B_i} \lambda_S^{-S_i} \lambda_Q^{-Q_i} \lambda_C^{-C_i} \lambda_b^{-b_i}.$$

In addition to the fugacities already introduced, we include γ_s, γ_c and γ_b raised to the power $-|S_i|$, $-|C_i|$ and $-|b_i|$ (with $|S_i|$, $|C_i|$ and $|b_i|$ the number of strange, charm and bottom and anti-strange, anti-charm and anti-bottom quarks in hadron species i respectively), to allow for possible incomplete equilibration in the strange, charm and bottom sectors [34]. In Eq.(3) quantum statistics is taken into account. In the Boltzmann approximation, the density can be calculated analytically in the form of a second order modified Bessel function of the second kind

$$n_i(T, \{\mu\}, \{\gamma\}) = \frac{g_i}{2\pi^2} m_i^2 T \lambda_T^{-1} \gamma_T^{-1} K_2 \left(\frac{m_i}{T} \right). \tag{4}$$

Since the use of quantum statistics requires numerical integration (or an evaluation of infinite sums), while Boltzmann statistics can be implemented analytically, it is advisable to identify those regions in which quantum statistics deviate greatly from Boltzmann statistics. In most applications of the statistical thermal model, only a small region of the $\mu - T$ parameter space is of interest. From the freeze-out condition [26], it is evident for pions quantum statistics must be implemented at all but the highest energies, while, for kaons, the deviation peaks at between 1 and 2%. For all other mesons,

the deviation is below the 1% level. For baryons, the deviation is extremely small for all except the nucleons at small $\sqrt{s}$.

Numerically, when quantum statistics are used, care has to be taken to exclude Bose-Einstein condensation. The Bose-Einstein distribution function diverges if,

$$e^{\beta(m_i - \mu_i)} \leq 1. \tag{5}$$

Such Bose-Einstein condensation doesn't happen, provided that the chemical potentials of all bosons included in the resonance gas are less than their masses (i.e. $\mu_i < m_i$)[26].

The chemical potentials μ_S, μ_Q, μ_C and μ_b are typically constrained in applications of the model by the initial strangeness, baryon-to-charge ratio, charm and bottom.

0.3 Extended THERMUS Particle Set

As mentioned earlier, in the extended particle data table (2008 particle data table), the charm and bottom hadrons are included. Thus, we will make a comparison with the previous THERMUS particle data table (2002 particle data table). When we look at the number of states for the two particle data tables as shown in Figs. 1 and 2 respectively, we count how many resonances exist in the intervals $(0, 0.2), (0.2, 0.4), (0.4, 0.6), ..., (10.0, 11.1)$ GeV and then plot these numbers with respect to mass (the mass is defined as the center of the interval).

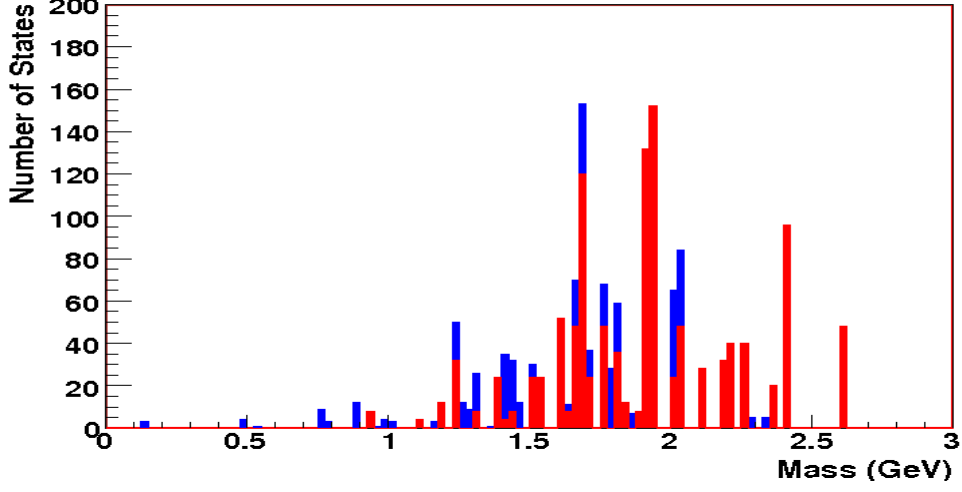**Figure 1:** The number of states for hadron particle data table arranged in terms of their masses, included are baryons (red) and mesons (blue) with u, d and s quarks up to 2.6 GeV, $N(2600)^+$ `$THERMUS/particles/PartList_PPB2002.txt` [26].
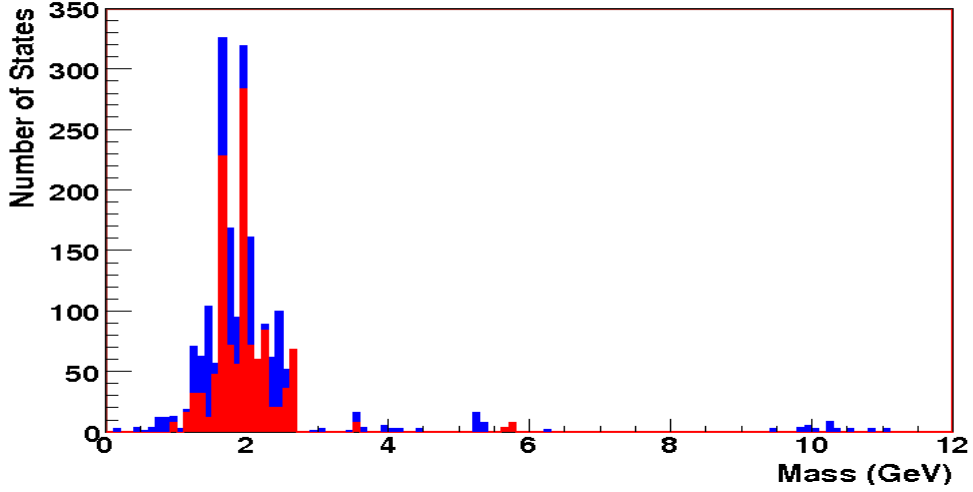

Figure 2: The number of states for particle data table arranged in terms of their masses. This is the updated THERMUS particle data table, it includes the c and b quarks up to 11.019 GeV, $\Upsilon(11020)^0$ `$THERMUS/extended_particles/PartList_PPB2008_CB.txt` (blue: mesons, red: baryons).

In addition to the first method, we presented in Figs. 1 and 2, to observe the difference between the two particle data tables and their number of states, also applied a second method to show their difference; that is, we add the

7

number of resonances in the intervals $(0, 0.2)$, $(0, 0.4)$, $(0, 0.6)$, ..., $(0, 11.1)$ GeV. Then, plot these numbers versus mass (the mass is defined as the center or the upper value of the interval) as shown in Fig. 3 and 4 respectively. These plots are clearer to notice the difference from the first method as we presented in Fig. 1.
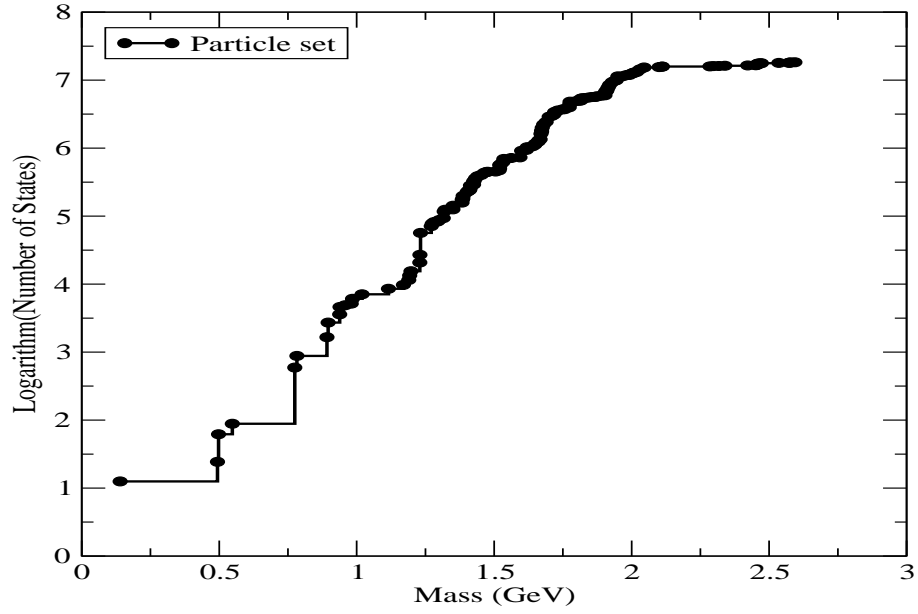

Figure 3: Logarithm of the number of states for particle data table which is found in $THERMUS/particles/PartList_PPB2002.txt [26] in terms of their masses.
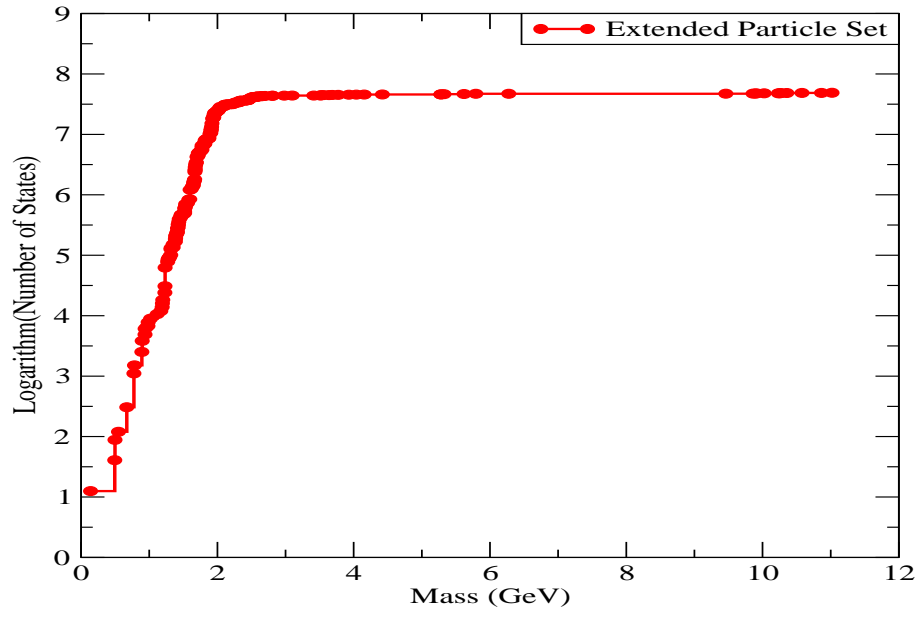
Figure 4: Logarithm of the number of states for particle data tables which is found in $THERMUS/extended_particles/PartList_PPB2008_CB.txt in terms of their masses.

From Figs. 2 and 4, the number of states and the corresponding logarithm increased from the previous particle data table. In Figs. 1 and 3, these changes come from the contributions of charm, bottom and newly included resonances in the 2008 particle data table. Furthermore, the empty gap as shown in Fig. 4 between 6 GeV - 9.5 GeV have not filled in by recent experiments. The responsible for this empty gap might be due to the detectors have seen those particles in order to fill in the empty gap. Based on these highlights, we will discuss the method to implement the extension of THERMUS based on the 2008 particle data table.

0.4   How to use The Extended THERMUS?

In this section, we will outline how to use THERMUS with the 2008 particle data table. Three distinct statistical ensembles are included in THERMUS, and the additional options to include quantum statistics, resonance width and excluded volume corrections are also available.

THERMUS has a default particle list which includes all mesons (up to the $\Upsilon(11020)^0$, previously, it was up to $K_4^*(2045)$) and baryons (up to the Ξ_b^0, previously, it was up to Ω^-) listed in the 2002 and 2008 Particle Physics Booklets [9, 35].

THERMUS has been tested using the 2008 particle data table and the decay files. The `TTMParticleSet` constructor now takes an additional argument `Bool_t CB_Included` which must be set to true. Here is the format with THERMUS a particular example of Ξ_b^- from 2008 particle data table:

```
root [1] TTMParticleSet
set("$/THERMUS/extended_particles/PartList_PPB$2008$_CB.txt",true)
root [2] set.InputDecays("$/THERMUS/extended_particles/",true)
root [3] TTMParticle *part = set.GetParticle(5232)
root [4] part->List()
```

```
********* LISTING FOR PARTICLE Xib- *********

 ID   = 5232   // Particle ID

 Deg. = 2       // degeneracy

 STAT = 1       // Fermi-Dirac statistics

 Mass      = 5.7924 GeV
 Width     = 0 GeV
 Threshold = 0 GeV

 Hard sphere radius = 0

 B =  1                          // B = Baryon
 S = -1            |S| = 1       // S = Strange
 Q = -1                          // S = Charge
 Charm  = 0        |C| = 0       // C = Charm
 Beauty = -1       |b| = 1       // b = Beauty
 Top    = 0        |T| = 0       // T = Top
            STABLE
************************************************
```

The first line, `root [1]` loads the 2008 particle data table; the second line, `root[2]` loads the input decays of the 2008 particle data list. The third, `root [3]` and fourth, `root [4]` can get particles from the 2008 particle data table and lists the particle respectively [26]. The latest version of the THERMUS package with both particle data tables is found in this link: `http://www.phy.uct.ac.za/courses/ staffwebsites/wheaton/THERMUS/SourceDownload.html`.

0.5 Results and Discussions

This section presents results based on the 2008 particle data table and makes comparisons with results obtained using the 2002 particle data table. Note that the 2008 particle data table has not yet been implemented to be used for the other two

ensembles, (the canonical and strangeness-canonical ensembles). In this chapter, all calculations use the grand-canonical ensemble.

The emphasis of our investigation is to establish quantitatively the similarities and differences in the production and contributions of particles observed in the elementary and heavy ion collisions. In the following subsection using THERMUS, we will discuss and analyze hadron particle yields and ratios as well as obtain the corresponding thermodynamic parameters with both particle data tables based on THERMUS fit.

0.5.1 Thermodynamic Parameters Analysis

We analyze the RHIC [36, 37, 38, 39] and LHC [11, 12, 13] results using THER-MUS, and compare the results for both particle data tables. THERMUS fits the experimental data in order to obtain the thermodynamic parameters.

We present results from the STAR experiment for Au-Au collisions at 130 and 200 GeV. The data has been used and analyzed previously in [40, 41, 10]. Our results using the STAR densities at mid-rapidity for various hadron species in the centrality region $(0 - 6\%)$ for Au-Au collisions at 130 GeV are shown in Fig. 5 (a) and (b). Similarly, the results at 200 GeV are shown in Fig. 6 (a) and (b). In these figures, the $K^{\pm}$, p, and $\bar{p}$ yields are given in [36, 37], while all other particles are derived from the measured values by *centrality interpolations* [2] described in reference [10] Section II A; these are $\pi^{\pm}$, ϕ, Λ, $\bar{\Lambda}$, Ξ^{-} and $\bar{\Xi}^{+}$.

Similarly, Fig. 6 (a) and (b) show STAR rapidity densities of various hadrons in Au-Au collisions at 200 GeV at centrality $(0 - 6)\%$ [10]. The experimentally measured values have been obtained from references [39, 42, 43]. The STAR data for p and $\bar{p}$ rapidity densities also include weak feeding from (multi-)strange hyperons [39]. The comparison between the model and STAR particle yields are presented in Figs. 5 and 6.

---

[2]Particle rapidity densities are sometimes measured in specific centrality windows which are different for various experiments. Hence, to perform an appropriate analysis of the full data set, one has to find a proper method in order to estimate rapidity densities for various hadronic species *in the same centrality* window.
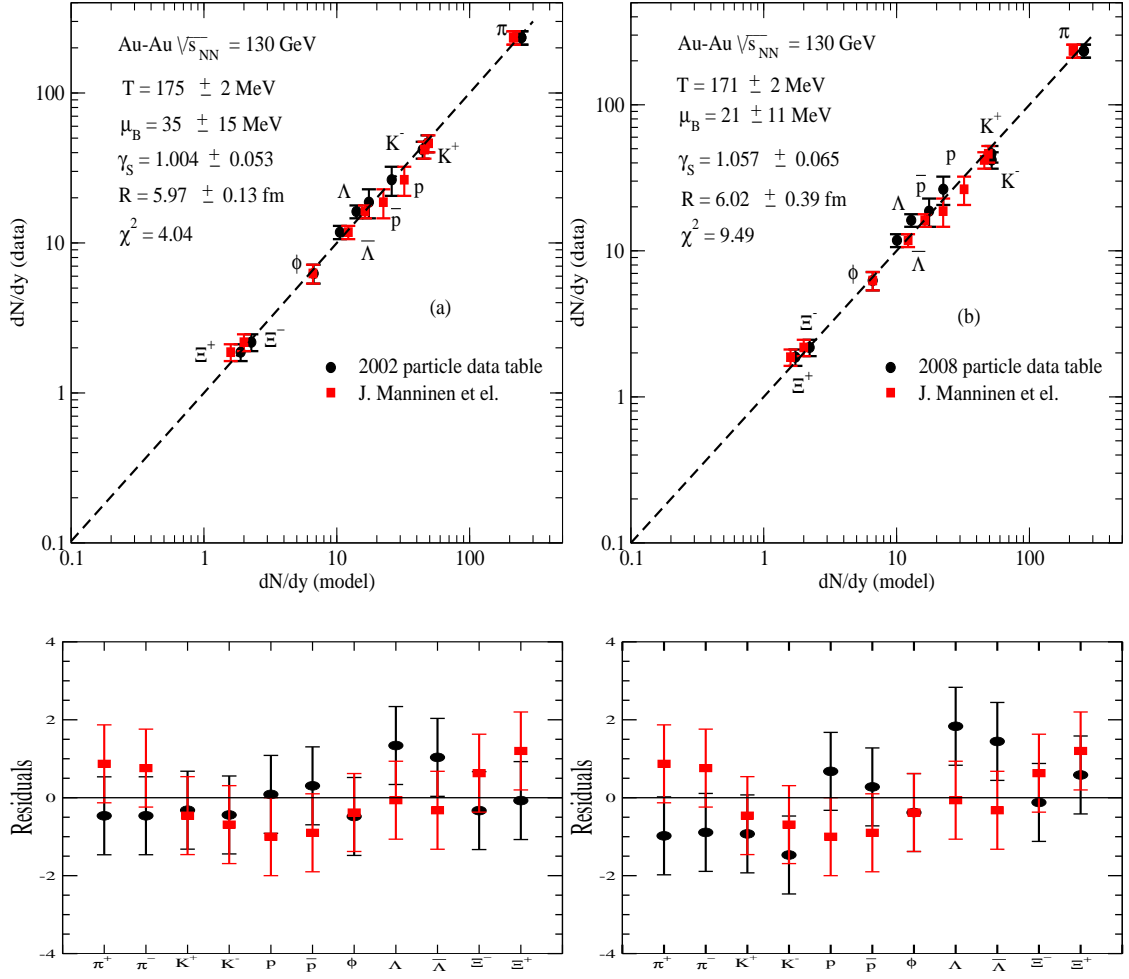
Figure 5: Figure (a) and (b) showing the comparison between rapidity densities in the combined fit and rapidity densities measured by STAR [10] for central Au-Au collision at 130 GeV and the corresponding thermal fit parameters are given for both particle data tables. Similarly, the comparison between rapidity densities in the combined fit and rapidity densities in terms of the residuals are presented for both particle data tables.

As presented in Fig. 5, THERMUS fits very well compared to [10]. However, the Λ's were underestimated by 16% compared to [10]. Similarly, Fig. 6 fits very well the STAR data [10] except ϕ's were underestimated by 18%. We have compared particle yields between the experimental and model fit values using the residual statistics [10].
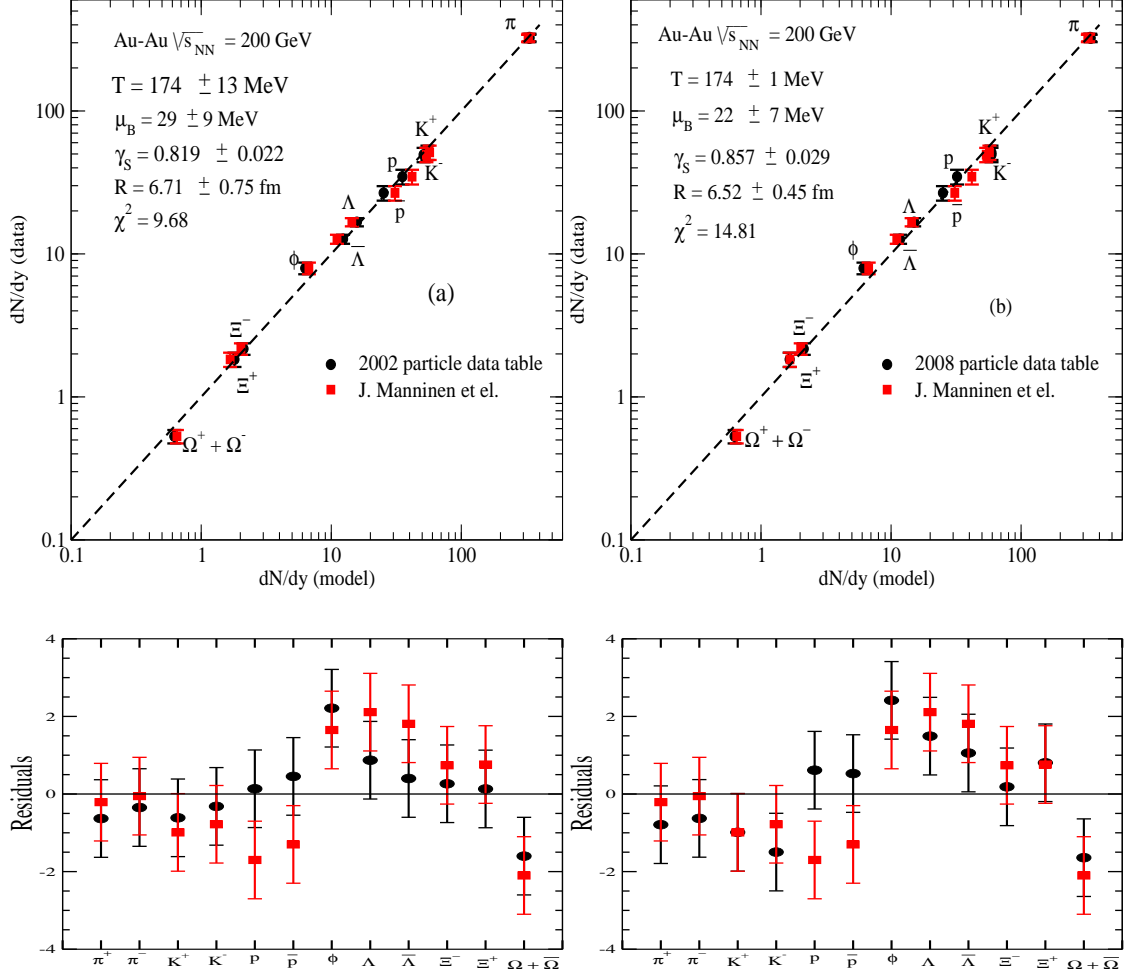
Figure 6: Figure (a) and (b) showing the comparison between rapidity densities in the combined fit and rapidity densities measured by STAR [10] for central Au-Au collision at 200 GeV and the corresponding thermal fit parameters are given for both particle data tables. Similarly, the comparison between rapidity densities in the combined fit and rapidity densities in terms of the residuals are presented for both particle data tables.

The residual is defined as the ratio between the difference in Experiment (E) and Model (M) value and the experimental error value (R), i.e.,

$$\texttt{Residual} \equiv \frac{\texttt{E} - \texttt{M}}{\texttt{R}}. \tag{6}$$

Using Eq. (6), we compare the particle yield results for both particle data tables with the experimental results for Au-Au collisions at 130 GeV and 200 GeV. The results are presented in Figs. 5 and 6.

14

The available data from RHIC experiment for Au-Au collisions at 130 GeV and 200 GeV [10] were compared with THERMUS. The particle yields for various hadron species and the thermodynamic parameters are given for both particle data tables in Figs. 5 and 6. The Fits to STAR data at 130 and 200 GeV show almost no difference between the experiment and THERMUS. Furthermore, we have removed some hadron species (for example Λ's and ϕ) from the fits in order to obtain a best fit; and the resulting fit thermodynamic parameters were modified slightly within the errors of the parameters.

According to results in Figs. 5(b) and 6(b), the results obtained with the 2008 particle data table show smaller freeze-out temperatures than the 2002 particle data table. Clearly, this is caused by increasing the radius of the system, which then causes a decrease of the freeze-out temperature. Thus, the variation of the radius obtained from the fit contributes greatly to the difference between the two particle data tables. This also makes a contribution to changing the freeze-out temperature and other thermodynamic parameters. In addition, THERMUS best fit parameters at chemical freeze-out results are different from [10].

In general, the results presented in Figs. 5 and 6, THERMUS overestimates most of the particle yields and underestimates Λ and ϕ yields at 130 and 200 GeV; THERMUS fits the experimental particle yield very well, in addition, we presented the residual analysis for both particle data tables and compared with experimental values in Figs. 5 and 6. Most of our residual results are in the range -1 to 1 within the error bar; therefore, THERMUS results give a better fit to the RHIC experimental data than those explained in [10].

Based on the ALICE central rapidity densities for the p-p collisions at 900 GeV and 7 TeV [11, 12, 13] for different hadron species, the corresponding predicted values are shown in Figs. 7 and 8. Based on the results shown in the Figs. 7 and 8, we noticed that the thermal fit parameters were also different for both particle data tables. However, the predicted particle ratios show similar results for both particle data tables.
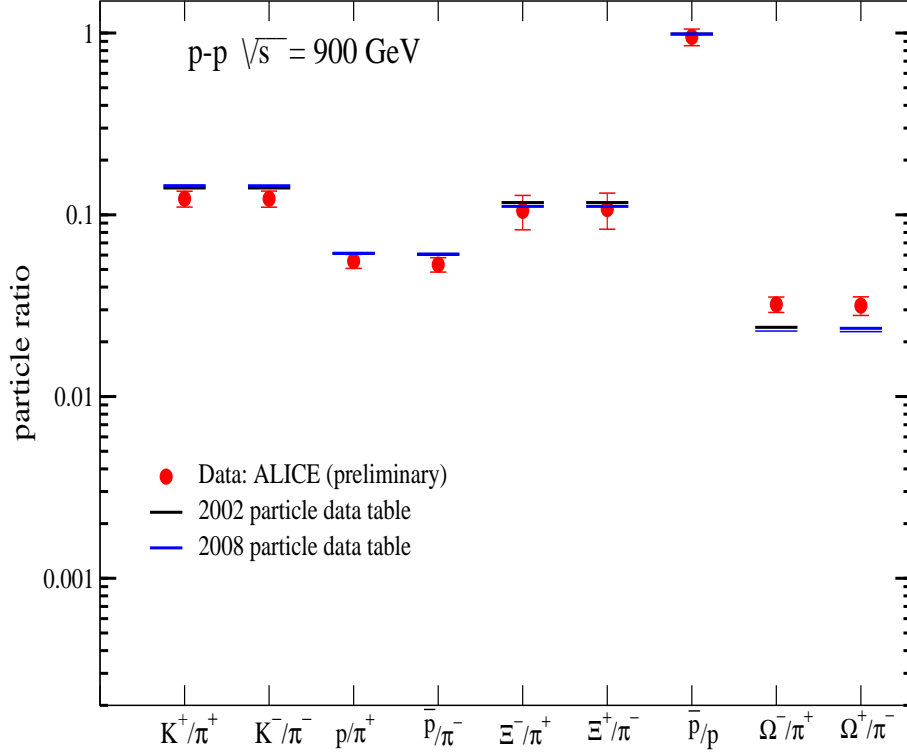
15

Figure 7: Particle yield results using the two particle data tables for the rapidity densities of the preliminary measured results from ALICE [11, 12, 13] for central p-p collision at 900 GeV. The thermal fit parameters are listed in Table 1.

Our results are presented in Figs. 7 and 8 for the particle ratios of the preliminary LHC results of the p-p collisions at 900 GeV and 7 TeV. The corresponding fitted thermodynamic parameters are listed in Tables 1 and 2. In conclusion, the thermal fit results from p-p collisions at 900 GeV and 7 TeV are in good agreement with THERMUS. The particles containing strangeness particles such as Ξ/π, Ω/π and Ω/Ξ were not fitted well compared to other particle ratios.

The particle yields for the preliminary measured results of the heavy ion experiment, Pb-Pb collision at 2.76 TeV [13] were calculated using THERMUS. The calculated particle ratios for different hadron species are presented in Fig. 9. Based on the results shown in Fig. 9, the thermal fit parameters were different for both particle data tables. However, the predicted particle yields are similar.
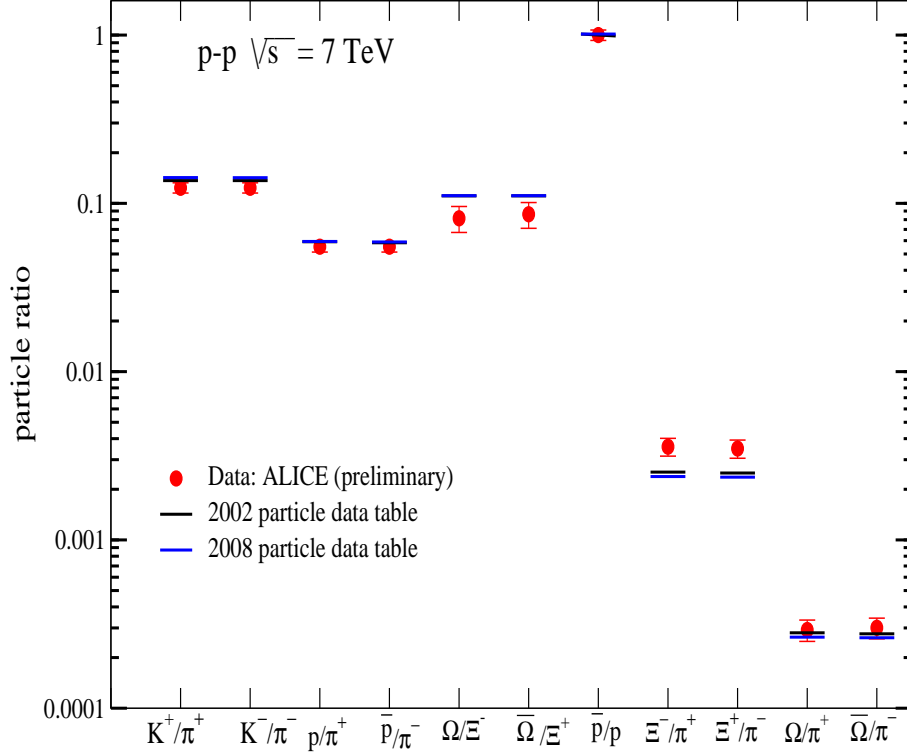
16

Figure 8: Particle yield results for the two particle data tables for the rapidity densities of the preliminary results by ALICE [11, 12, 13] for central p-p collision at 7 TeV. The fit results were obtained from THERMUS 2002 and 2008 particle data tables. The thermal fit parameters are listed in Table 2.

Table 1: The predicted thermal fit parameters for p-p collision at 900 GeV on ALICE [11, 12, 13]. The fit results were obtained from both THERMUS particle data tables (where THERMUS 2002 particle data table, Fit (2002) and THERMUS 2008 particle data table, Fit (2008)).

Parameters	Fit (2002)	Fit (2008)
T (GeV)	0.152 ± 0.002	0.154 ± 0.002
μ_B (GeV)	0.001 (fixed)	0.001 (fixed)
μ_S (GeV)	0.0	0.0
μ_Q (GeV)	0.0	0.0
γ_s	0.733 ± 0.041	0.707 ± 0.042

Similarly, using the preliminary particle yield results for Pb-Pb collision at 2.76 TeV [12, 13]; we have presented our fit results in Fig. 9. The fitted thermodynamic parameters are listed in Table 3. In addition, the thermal fits are in good agreement

17

Table 2: The predicted thermal fit parameters for p-p collision at 7 TeV on ALICE [11, 12, 13]. The fit results were obtained from the two particle data tables.

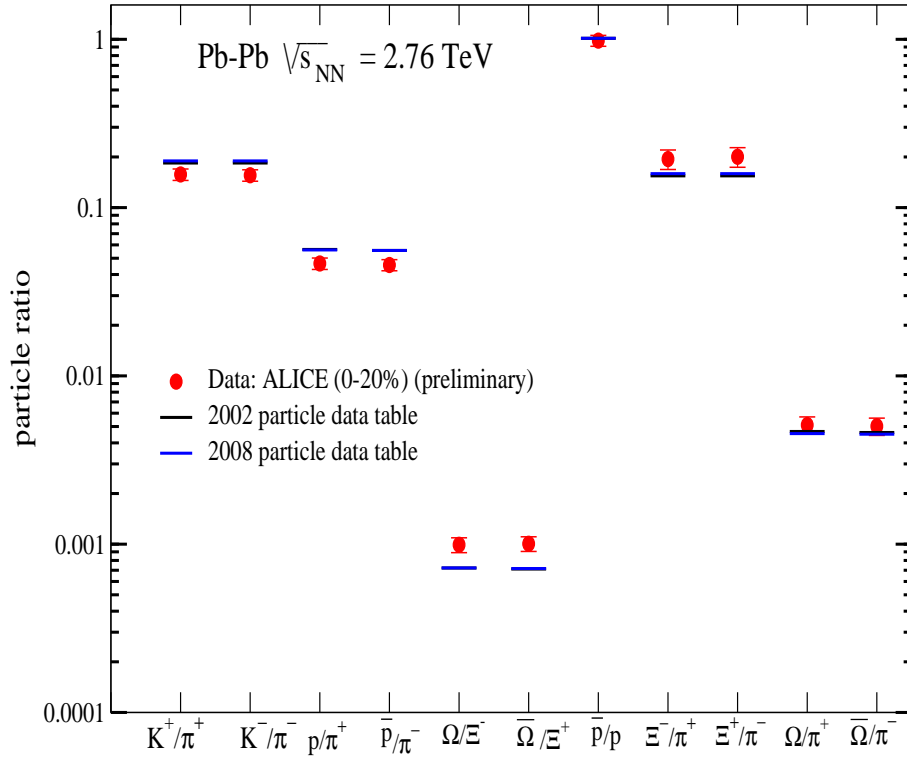| Parameters	Fit (2002)	Fit (2008)
T (GeV)	0.150 ± 0.002	0.152 ± 0.002
μ_B (GeV)	0.001 (fixed)	0.001 (fixed)
μ_S (GeV)	0.0	0.0
μ_Q (GeV)	0.0	0.0
γ_s	0.714 ± 0.023	0.697 ± 0.023

Figure 9: Particle yield results using two particle data tables for the rapidity densities from ALICE in central Pb-Pb collision at 2.76 TeV [12, 13].

between the THERMUS and the preliminary results for all particles containing strangeness such as kaons and hyperons.

The recent experimental results at LHC for p-p collisions at 900 GeV and 7 TeV as well as Pb-Pb collision at 2.76 TeV [11, 12, 13] have been analyzed using

Table 3: The predicted thermal fit parameters for Pb-Pb collision at 2.76 TeV on ALICE [12, 13]. The fit results were obtained from both THERMUS particle data tables.

Parameters	Fit (2002)	Fit (2008)
T (GeV)	0.150 ± 0.001	0.152 ± 0.001
μ_B (GeV)	0.001 (fixed)	0.001 (fixed)
μ_S (GeV)	0.0	0.0
μ_Q (GeV)	0.0	0.0
γ_s	1.0 (fixed)	1.0 (fixed)

THERMUS. We have used preliminary results and analyzed the corresponding thermodynamic parameters from particle yield results. The fitted thermodynamic parameters are presented in Figs. 7, 8 and 9; the corresponding fitted thermodynamic parameters are given Tables 1, 2 and 3.

The thermal parameters obtained with the THERMUS fit to the experimental data for p-p and Pb-Pb collisions are stable in some ranges. In particular, the freeze-out temperature is between 150 MeV and 175 MeV while the beam energy changed over several orders of magnitude. This occurred over a wide range of energies, different collision systems and parameters. The freeze-out temperature, strangeness saturation factor, radius, baryon chemical potential and strangeness chemical potential have been well parameterized with small uncertainties. They have also been compared with [5, 44] as a function of energy. In many ways, this remarkable success in describing the data with a few simple statistical parameters can be viewed as an indication that the particles in these collisions were indeed produced in a thermally and chemically equilibrated system.

0.6   Summary

We have analyzed and discussed the hadron abundances measured in Au-Au, p-p and Pb-Pb collisions at RHIC and LHC experiments using THERMUS; our results for hadron abundances are in agreement with a thermally equilibrated system. The results were obtained with the 2002 and 2008 particle data tables and their differences have been explained in this chapter. In particular, the data from the RHIC experiment for Au-Au collisions at 130 GeV and 200 GeV have been

discussed and analyzed. Similarly, using the preliminary particle ratios result in p-p collisions at 0.9 TeV and 7 TeV as well as Pb-Pb collision at 2.76 TeV, the particle yield predictions and thermodynamic parameters obtained from the fits have been presented.

THERMUS has also been used to describe the particle ratios using the two particle data tables. The 2008 particle data table can be used to perform more analysis of particle ratios for lighter and heavier hadron masses obtained from elementary and heavy ion collisions [9]. We have analyzed our results using the previous freeze-out curve parameters [5, 45, 46] for 2008 particle data table. Thus, THERMUS needs a new recalculation of the freeze-out curve in order to obtain a better thermal fit results than the present ones.

References

[1] R. Hagedorn. Statistical thermodynamics of strong interactions at high- energies. *Nuovo Cim. Suppl.*, 3:147–186, 1965.

[2] R. Hagedorn. *Riv. Nuovo Cimento*, **6**(10), 1984.

[3] R. Hagedorn. Hadronic matter near the boiling point. *Nuovo Cim.*, 56A:1027–1057, 1968.

[4] J. Cleymans and K. Redlich. Chemical and thermal freeze-out parameters from $1A$ to $200A$ `GeV`. *Phys. Rev. C*, 60:054908, Oct 1999.

[5] J. Cleymans, H. Oeschler, K. Redlich, and S. Wheaton. Comparison of chemical freeze-out criteria in heavy-ion collisions. *Phys. Rev.*, C73:034905, 2006.

[6] S. Chatterjee, R. M. Godbole, and Sourendu Gupta. Stabilizing hadron resonance gas models. *Phys. Rev.*, C81:044907, 2010.

[7] Wojciech Broniowski, Wojciech Florkowski, and Leonid Ya. Glozman. Update of the Hagedorn mass spectrum. *Phys. Rev. D*, 70(11):117503, Dec 2004.

[8] S. Wheaton, J. Cleymans, and M. Hauer. THERMUS: A Thermal model package for ROOT. *Comput.Phys.Commun.*, 180:84–106, 2009, http://www.phy.uct.ac.za/courses/staffwebsites/wheaton/THERMUS/thermus_index.html.

[9] Claude Amsler et al. Review of particle physics. *Phys. Lett.*, B667:1–1340, 2008.

[10] J. Manninen and F. Becattini. Chemical freeze-out in ultra-relativistic heavy ion collisions at $\sqrt{s_{NN}} = 130$ and 200 `GeV`. *Phys. Rev.*, C78:054901, 2008.

[11] K. Aamodt and others (ALICE Collaboration). Production of pions, kaons and protons in p-p collisions at $\sqrt{s}=$ 900 `GeV` with ALICE at the LHC. *Eur. Phys. J.*, C71:1655, 2011.

[12] M. Floris and for the ALICE Collaboration. Identified particles in p-p and Pb-Pb collisions at LHC energies with the ALICE detector. *J.Phys.G*, G38:124025, 2011.

[13] A. Kalweit (ALICE Collaboration). Global properties of strange particle production in p-p and pb-pb collisions with the alice detector. *Talk presented at SQM2011, Cracow, Poland.*

[14] R. Brun and F. Rademakers. ROOT-An Object Oriented Data Analysis Framework, ROOT web page, `http://root.cern.ch/`. *Nucl. Inst. & Meth. in Phys. Res. A*, 389:81, 1997.

[15] W. Broniowski W. Florkowski J. Letessier G. Torrieri, S. Steinke and J. Rafelski. SHARE: Statistical hadronization with resonances. *Comput. Phys. Commun.*, 167, 2005.

[16] Adam Kisiel, Tomasz Taluc, Wojciech Broniowski, and Wojciech Florkowski. Therminator: Thermal heavy-Ion generator. *Comput. Phys. Commun.*, 174:669, 2006.

[17] J. Cleymans and K. Redlich. Unified description of freeze-out parameters in relativistic heavy ion collisions. *Phys. Rev. Lett.*, 81:5284–5286, 1998.

[18] P. Braun-Munzinger and J. Stachel. Probing the Phase Boundary between Hadronic Matter and the Quark-Gluon-Plasma in Relativistic Heavy Ion Collisions. *Nucl.Phys.A*, 606:320, 1996.

[19] P Braun-Munzinger and J Stachel. Particle ratios, equilibration and the QCD phase boundary. *Journal of Physics G: Nuclear and Particle Physics*, 28(7):1971, 2002.

[20] A Tawfik. Influence of strange quarks on the QCD phase diagram and chemical freeze-out. *Journal of Physics G: Nuclear and Particle Physics*, 31(6):S1105, 2005.

[21] J. Cleymans, M. Stankiewicz, P. Steinberg, and S. Wheaton. The origin of the difference between multiplicities in e^+e^- annihilation and heavy ion collisions. eprint:nucl-th/0506027, 2005.

[22] A. Tawfik. On the conditions driving the chemical freeze-out. *Europhys. Lett.*, 75:420, 2006.

[23] V. Magas and H. Satz. Conditions for confinement and freeze-out. *The European Physical Journal C - Particles and Fields*, 32:115–119, 2003. 10.1140/epjc/s2003-01375-1.

[24] J. Cleymans and D. Worku. The Hagedorn temperature Revisited. *Mod. Phys. Lett.*, A26:1197–1209, 2011.

[25] P. Castorina, J. Cleymans, D. E. Miller, and H. Satz. The Speed of Sound in Hadronic Matter. *Eur. Phys. J.*, C66:207–213, 2010.

[26] S. Wheaton. The development and application of `THERMUS- a Statistical-Thermal Model Analysis Package for ROOT`. *Ph.D. thesis, University of Cape Town*, Cape Town, South Africa, 2005.

[27] K. Redlich, J. Cleymans, H. Oeschler, and A. Tounsi. Particle production and equilibration in heavy ion collisions. *Acta Phys. Polon.*, B33:1609–1628, 2002.

[28] F. Becattini, J. Cleymans, A. Keranen, E. Suhonen, and K. Redlich. Features of particle multiplicities and strangeness production in central heavy ion collisions between 1.7A and 158A `GeV`/c. *Phys.Rev.C*, 64:024901, 2001.

[29] P. Braun-Munzinger, I. Heppe, and J. Stachel. Chemical Equilibration in Pb-Pb Collisions at the SPS. *Phys.Lett.B*, 465:15, 1999.

[30] P. Braun-Munzinger, J. Stachel, J. P. Wessels, and N. Xu. Thermal Equilibration and Expansion in Nucleus-Nucleus Collision at the AGS. *Phys.Lett.B*, 344:43, 1995.

[31] Wojciech Broniowski and Wojciech Florkowski. Strange particle production at RHIC in a single-freeze-out model. *Phys. Rev. C*, 65:064905, 2002.

[32] M. Kaneta and N. Xu. On chemical equilibrium in high-energy heavy-ion collisions. *J. Phys. G: Nucl. Part. Phys.*, 27:589, 2001.

[33] M. Kaneta (for the NA44 Collaboration). Particle ratios from central Pb-Pb collisions at the CERN SPS. *J. Phys. G:Nucl. Part. Phys.*, 23:1865, 1997.

[34] Jean Letessier, Johann Rafelski, and Ahmed Tounsi. Gluon production, cooling and entropy in nuclear collisions. *Phys.Rev.C*, 50:406, 1994.

[35] F. Becattini, J. Manninen, and M. Gazdzicki. Energy and system size dependence of chemical freeze-out in relativistic nuclear collisions. *Phys.Rev.*, C73:044905, 2006.

[36] J. Adams *et al.* [STAR Collaboration]. Kaon Production and Kaon to Pion Ratio in Au-Au Collisions at $\sqrt{s_{NN}} = 130$GeV. *Phys. Lett. B*, 595:143, 2004.

[37] J. Adams *et al.* [STAR Collaboration]. Rapidity and centrality dependence of proton and antiproton production from Au-Au collisions at $\sqrt{s_{NN}} = 130$GeV . *Phys. Rev. C*, 70(4):041901, Oct 2004.

[38] J. Adams *et al.* [STAR Collaboration]. Identified Particle Distributions in p-p and Au-Au Collisions at $\sqrt{s_{NN}} = 200$ GeV. *Phys. Rev. Lett.*, 92(11):112301, Mar 2004.

[39] J. Adams *et al.* [STAR Collaboration]. Scaling Properties of Hyperon Production in Au-Au Collisions at $\sqrt{s_{NN}} = 200$ GeV. *Phys. Rev. Lett.*, 98(6):062301, Feb 2007.

[40] J. Cleymans, B. Kampfer, M. Kaneta, S. Wheaton, and N. Xu. Centrality dependence of thermal parameters deduced from hadron multiplicities in Au-Au collisions at $\sqrt{s_{NN}} = 130$ GeV. *Phys.Rev.C*, 71:054901, 2005.

[41] Nu Xu and Masashi Kaneta. Hadron freeze-out conditions in high energy nuclear collisions. *Nucl. Phys. A*, 698:306, 2002.

[42] B. I. Abelev *et al.* [STAR Collaboration]. Partonic Flow and ϕ-Meson Production in Au-Au Collisions at $\sqrt{s_{NN}} = 200$ GeV. *Phys. Rev. Lett.*, 99(11):112301, Sep 2007.

[43] J. H. Chen. System size and energy dependence of ϕ meson production at RHIC. *J. Phys. G*, 35:104053, 2008.

[44] A. Andronic, P. Braun-Munzinger, and J. Stachel. Thermal hadron production in relativistic nuclear collisions: The Hadron mass spectrum, the horn, and the QCD phase transition. *Phys.Lett.*, B673:142–145, 2009.

[45] A. Andronic, P. Braun-Munzinger, and J. Stachel. Hadron production in central nucleus nucleus collisions at chemical freeze-out. *Nucl. Phys.*, A772:167–199, 2006.

[46] F. Becattini, J. Manninen, and M. Gaździcki. Energy and system size dependence of chemical freeze-out in relativistic nuclear collisions. *Phys. Rev. C*, 73(4):044905, Apr 2006.